THE DEEP STRUCTURE OF A COLLAPSED CENTRAL UPLIFT – INSIGHTS IN THE DEVELOPMENT OF THE VREDEFORT DOME, SOUTH AFRICA. A. Jahn[1] and U. Riller[2], [1]Museum für Naturkunde – Leibniz Institute at the Humboldt University Berlin, Invalidenstrasse 43, D-10115 Berlin, Germany (Andreas.Jahn@mfn-berlin.de), [2]McMaster University, 1280 Main Street West, Hamilton, ON, L8S 4K1, Canada.

Introduction: In order to investigate the subsurface structure of the Vredefort Dome (Fig.1), the central uplift of the Proterozoic Vredefort impact structure (2.02 Ga), structural, petrological and geophysical work [1, 2, 3], as well as numerical modeling [4], have been conducted. Based on these studies and new ground data, we constructed a 3D structural model for the upper parts of the central uplift. This model offers new insights in the structural inventory of tilted sedimentary rocks and the fault system of the collar. Our modeling results are consistent with an impact-induced suite of normal and reverse faults in this area and allows to link them to distinct stages of rock movements during the modification phase.

The Vredefort Dome is the deeply eroded remnant of the collapsed central uplift structure [1]. The inner core of the Dome is approximately 40 km in diameter and consists mainly of Archean (> 3.1 Ga) granitoids and minor mafic intrusions. It is surrounded by the collar, an assembly of steeply dipping and overturned sedimentary and volcanic strata of Archean and Paleoproterozoic (3.07 - 2.1 Ga) age. To the north and west, the collar rocks are well exposed and form a series of concentric, morphologically prominent quartzite ridges, and valleys along less resistant shale horizons, wrapping around the crystalline core. To the east and the south, the central uplift is largely covered by the Phanerozoic Karoo Supergroup and Quaternary deposits.

Methods: In field campaigns in 2007 and 2008 we collected structural data, predominantly in the northern and western collar region, and created a detailed map of bedding plane orientations and faults identifiable in outcrop. In combination of surface structural data, seismic data and information from drill holes we constructed a 3D model of the respective collar strata with the software *ArcGIS* and *GOCAD* (Fig.2). For the visualization of the rock orientations we chose prominent lithological interfaces within the Archean sediments (upper and lower boundary of the Central Rand Group, Witwatersrand Supergroup) as marker surfaces. We also included a number of prominent dislocations known from previous field studies [6] and geophysical imaging. In order to test the plausibility of our results, we compared them to those of predicted by numerical models [3].

The construction of a 3D multi-surface model characterized by impact-induced faults allowed us to identify coherent rock domains and to determine their minimum displacements during collapse of the central uplift. Changes in the dips of strata with depth were analysed as well as the influence of topography and spatial distribution on these values.

The model is limited by the exposure of pre-impact (meta)sedimentary rocks and, therefore, to the northern and western quadrants of the central uplift.

Results: The dips of inclined to steeply dipping, overturned sedimentary strata in the collar region increase from < 60° to 70-90° at a depth of 2 to 3 km. Their total amounts of rotation reach up to 150°. Hence, the current erosion surface is situated within the hinge zone between the steeply dipping strata and the overturned parts in the roof of the collapsed central uplift [4]. This observation of a transition zone agrees with erosion of 6 to 8 km. The dip of bedding planes also varies with the individual domains defined by faults. Generally, the bedding planes display maximal rotations in the northwest, but this may be blurred by differential rotation between adjacent domains and topographic effects.

On the km-scale, a significant number of faults is exposed in the collar. With respect to the center of the Vredefort Dome, most of them are either concentric [5] or radial faults [6]. Concentric faults strike parallel to the outcrop lines of strata, but intersect the strata. Thus, thicknesses of strata are reduced by movements on concentric faults. Radial faults, however, are more curved at surface, listric in geometry and displace concentric faults. The displacement values range from a few hundred meters to 2 km and decline with distance from the core.

Conclusions: Our field structural analysis revealed the existence of a set of faults with variable orientations and truncation relationships. The observed fault geometry supports the hypothesis of a complex impact-related fault system comprising normal and reverse faults in a close genetic context.

The geometry and geometric relationship of bedding and fault surfaces point to impact-induced deformation. The shape and orientation of the faults with respect to orientation of bedding planes excludes an origin of the faults in their current orientation. Concentric faults formed likely by reverse sense of slip toward the crater center and appear to be younger than the collapse of the central uplift. By contrast concentric faults are displaced by radial ones, which were tilted later. Consequently, the concentric faults must have formed during an early stage of crater modification.

Back rotation of the collar strata to their pre-impact orientation leads us to the following kinematic model of faulting during central uplift formation.

Back rotation of the concentric faults by the same rotation magnitude as bedding planes, suggests an origin of these faults as normal faults. Thus, concentric faults are likely relics of discontinuities accomplishing terracing of the rim of the transient cavity (Fig. 3a). The geometry of concentric faults was subsequently modified by radial faults which formed as reverse or thrust faults. Overall, the fault kinematics point to a constrictional rock flow, which is compatible with the formation of the central uplift by crater-inward mass flow (Fig. 3b, c). As a consequence of convergent rock flow toward the crater center, the strata and faults were uplifted and rotated as well as displaced outwards with respect to the crater center (Fig. 3d).

References: [1] Reimold W.U. and Gibson R.L. (2006) *Chemie der Erde, 66,* 1–35. [2] Lana C. and Gibson R. L. (2006) *S. Afr. J. of Geol., 109,* 265-278. [3] Henkel H. and Reimold W.U. (2002) *J. of Applied Geophys.,* 43–62. [4] Ivanov B. (2005) *Solar System Research, 39,* 381-409. [5] Grieve R.A.F., Reimold W.U., Morgan J., Riller U. and Pilkington M. (2008) *Meteorit. Planet. Sci*., 43, 855-882. [6] Bisshoff A.A. and Mayer J.J. (1999), *Council for Geoscience, Pretoria*, Geol. Map 1:50.000.

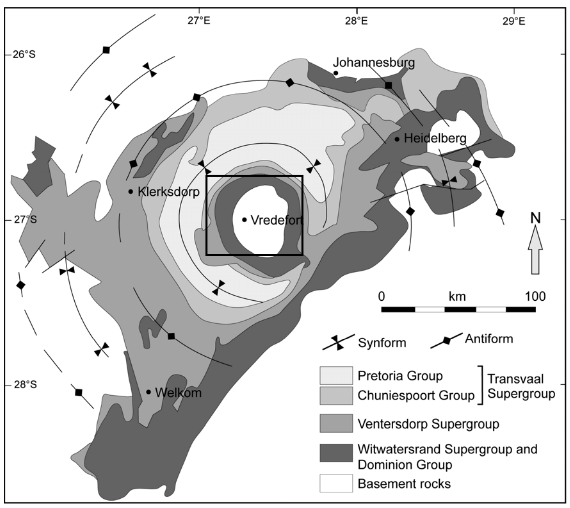

Fig. 1: Map of the Witwatersrand Basin. The centrally seated Vredefort Dome with its uplifted basement rocks and metasediments is structurally limited by the Potchefstroom Synclinorium. The box indicates the position of the model (Fig. 2).

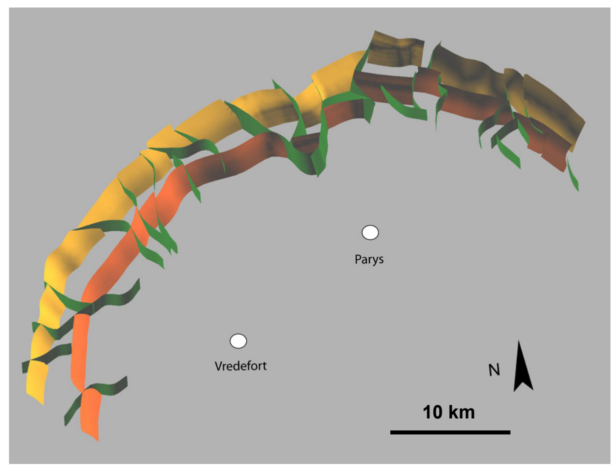

Fig. 2: 3D model of the upper (yellow) and lower (orange) boundary of the Central Rand Group (Witwatersrand Supergroup). The model was constructed with GoCad 2.1.6. The vertical extent is 3km.

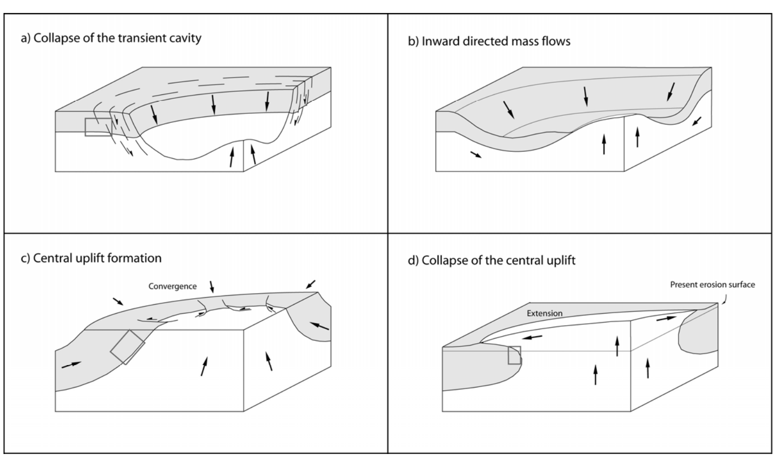

Fig. 3: Summary of succession of mass movements during the modification stage. Arrows indicate movement directions of rocks, boxes represent the recent level of exposure.
(a) Early modification phase: the rim of the transient cavity collapses. Besides listric terraces of the crater walls smaller concentric normal faults with listric shape develop. (b) Collapse of the crater rim: inward-directed mass flow contributes to the growth of the central uplift. (c) Convergent mass movements form a central uplift. Compression leads to the formation of reverse faults that become gradually rotated upwards. (d) The uplift growth reaches its vertical limit and the central peak begins to collapse outward, with the upper strata undergoing strong rotation.